

generated September 29, 2018

N(H I)/E(B-V)

Harvey Liszt

*National Radio Astronomy Observatory
520 Edgemont Road, Charlottesville, VA 22903-2475*

hliszt@nrao.edu

ABSTRACT

We explore the relationship between dust-emission derived reddening $E(B-V)$ and atomic hydrogen column density $N(\text{H I})$ derived from 21 cm emission surveys. We consider measurements at galactic latitude $|b| \gtrsim 20^\circ$ and $E(B-V) \lesssim 0.1$ mag where the interstellar gas is predominantly neutral and atomic and opacity corrections to 21cm H I profiles are small. Over the Galaxy at large at lower resolution in H I, and on smaller scales at higher resolution, we find that the reddening is always much smaller than would be expected from the usually-quoted relation $N(\text{H}) = 5.8 \times 10^{21} \text{ cm}^{-2} E(B-V)$ based on stellar reddening and uv absorption toward early-type stars. On wide scales, we find $N(\text{H I}) = 8.3 \times 10^{21} \text{ cm}^{-2} E(B-V)$. We cite various precedents for such a large $N(\text{H I})/E(B-V)$ ratio whenever wide-field 21cm emission surveys are considered, including when reddening based on galaxy counts or colors is substituted for the dust-emission derived reddening measure.

Subject headings: astrochemistry . ISM: dust . ISM: H I. ISM: clouds. Galaxy

1. Introduction

A linear relationship between optical reddening $E(B-V)$ and the total column density of hydrogen nuclei $N(\text{H}) = N(\text{H I}) + 2 N(\text{H}_2)$ is a cornerstone of modern astrophysics, with a widely-quoted constant of proportionality $N(\text{H}) = 5.8 \times 10^{21} \text{ cm}^{-2} E(B-V)$ derived from Ly- α and H_2 absorption against a small number of early-type stars using the *Copernicus* satellite (Bohlin et al. 1978; Savage et al. 1977). The same constant of proportionality is implicit in the definition of the “Standard” H I cloud of Spitzer (1968).

This relationship was at first extended over the sky using galaxy counts to measure optical extinction (Burstein & Heiles 1982) (BH82; see also Heiles (1976)) and more recently using far infrared (FIR) dust emission-derived measures from higher-resolution (6′) all-sky surveys (Schlegel et al. 1998) (SFD98). For the atomic hydrogen column density, the all-sky, stray radiation- corrected LAB 21cm H I emission survey (Kalberla et al. 2005) with 0.6° resolution on a 0.5° grid stands in for Ly- α absorption. MM-wave CO emission surveys (Dame et al. 2001; Abdo et al. 2010; Planck Collaboration et al. 2011) have been used as surrogates for H₂ at higher reddening $E(B-V) > 0.1$ mag where the H₂ fraction is appreciable (Savage et al. 1977) and N(H) necessarily diverges from N(H I). The H₂-fraction has also been estimated using $2N(\text{H}_2) = 5.8 \times 10^{21} \text{ cm}^{-2} E(B-V) - N(\text{H I})$ (Abdo et al. 2010; Liszt et al. 2010; Liszt & Lucas 2002), partly as a means of calibrating the so-called CO-H₂ conversion factor.

The subject of this work is the relationship between N(H I) derived from 21cm measurements and $E(B-V)$ at $0.02 \text{ mag} < E(B-V) < 0.1 \text{ mag}$. In this regime the H₂-fraction is small, the hydrogen is predominantly neutral and atomic and the optical depth in the 21 cm H I line is low. Thus all of the commonly-considered systematic errors in deriving N(H I) are minimized and there should be little difficulty in demonstrating the proportionality between N(H I) *cum* N(H) and $E(B-V)$. However, we find that the slope of the N(H I)- $E(B-V)$ relationship is very different from that expected, typically by about 40%, over large and small regions of the sky, at low and high spatial resolution, no matter which recent H I survey is considered.

The organization of this work is as follows. In Section 2 we describe our use of the various H I and reddening measures and databases. In Section 3 we show the N(H I)- $E(B-V)$ relationships that result. In Section 4 we discuss some recent and historical antecedents for adjusting the $E(B-V)/N(\text{H I})$ relationship and Figure 5 is a brief summary presenting the alternatives that suggest themselves for understanding the present results.

2. Observational material and empirical results

2.1. Reddening

For comparison with N(H I) we derived reddening values at the nearest pixel in the SFD98 datacubes (North and South) and made sure to check our values against those served online¹ given the unexpected nature of the plots we produced. The SFD98 datacubes present equivalents of the optical reddening $E(B-V)$ derived from far infrared dust emission at 6′ resolution on a 2.5′ pixel grid, with a stated error of 16% at each pixel. We also compared the SFD98 results with those

¹<http://irsa.ipac.caltech.edu/applications/DUST/>

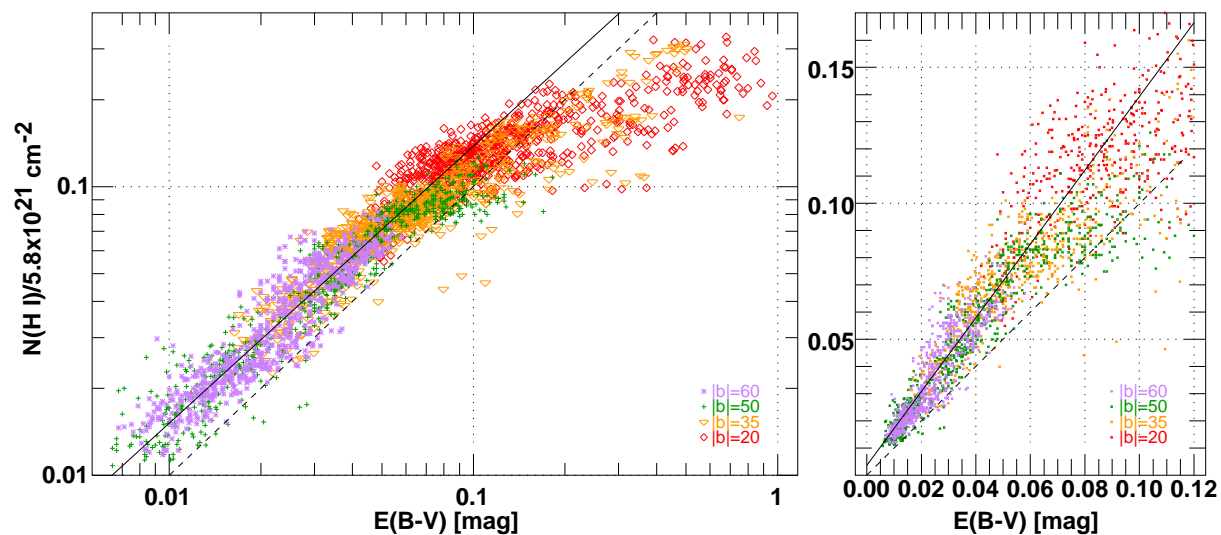


Fig. 1.— Reddening $E(B-V)$ from SFD98 and scaled LAB-survey H I column density $N(\text{H I})/5.8 \times 10^{21} \text{ cm}^{-2}$. $N(\text{H I})$ was derived assuming a spin temperature of 145 K to correct for optical depth. $N(\text{H I})$ and $E(B-V)$ were sampled at the grid points of the LAB survey, ie at even 0.5° intervals around the sky at galactic latitudes $b = \pm 20^\circ, \pm 35^\circ, \pm 50^\circ$ and $\pm 60^\circ$. The dashed line in each panel represents the canonical scaling of $E(B-V)$ and $N(\text{H I})$, the solid line is a regression fit. A handful of points at $E(B-V) > 1 \text{ mag}$ have been omitted in the left-hand panel. The right hand panel shows the data on a linear scale at smaller values of $E(B-V)$.

from the work of BH82, on the gridpoints of the latter, ie spaced 0.6° in galactic latitude and 0.3° in longitude.

2.2. 21cm H I

We derived $N(\text{H I})$ from brightness temperature profiles of 21cm radiation, lightly correcting for optical depth using a spin temperature of 145 K, which corresponds to the mean ratio of 21cm emission and absorption (Liszt et al. 2010) in the Millenium H I Emission-Absorption Survey of Heiles & Troland (2003). The correction to $N(\text{H I})$ for H I optical depth is never more than a few percent at $N(\text{H I}) < 5 \times 10^{20} \text{ cm}^{-2}$, $E(\text{B-V}) < 0.08$ mag where the disparity between the canonically-scaled $E(\text{B-V})$ and $N(\text{H I})$ is most clearly manifest. The upward correction for the possible contribution of ionized hydrogen is ignored here, but it would only exaggerate the effects that are discussed.

On large scales we used the LAB all-sky, stray-radiation corrected survey data (Kalberla et al. 2005) that has 0.6° spatial resolution on a pixel grid spaced 0.5° , with a velocity resolution of 1.3 km s^{-1} . We checked our profile integrals against those from the online LAB survey server ².

We also derived $N(\text{H I})$ over smaller regions using cubes of H I profiles from the GALFA-HI survey (Peek et al. 2011)³ that has $4'$ resolution on a $1'$ pixel grid with 0.8 km s^{-1} velocity resolution. We confirmed that the GALFA and LAB surveys are on the same intensity scale by synthesizing a few spectra at 0.6° resolution at positions corresponding to LAB survey pixels, using GALFA data.

3. Empirical results

3.1. Wide-angle results using the LAB H I survey

Figure 1 shows the results of plotting scaled values of $N(\text{H I})/5.8 \times 10^{21} \text{ cm}^{-2}$ vs $E(\text{B-V})$ from SFD98. We sampled around the entire sky at the 720 longitude gridpoints of the LAB survey, ie at even 0.5° intervals of galactic longitude at $b = \pm 20^\circ, \pm 35^\circ, \pm 50^\circ$ and $\pm 60^\circ$, to cover a wide range in $N(\text{H I})$ and $E(\text{B-V})$; we used the nearest datapoint in the $2.5'$ -pixel datacubes of SFD98. Figure 1 shows the data on a wider log scale at left and at smaller $E(\text{B-V})$ on a linear scale at right.

²<http://www.astro.uni-bonn.de/hisurvey/profile/>

³<https://purcell.ssl.berkeley.edu/>

The dashed lines in Figure 1 are the canonical scaling relationship $N(\text{H I})/5.8 \times 10^{21} \text{ cm}^{-2} = E(\text{B-V})$ which should hold at lower $E(\text{B-V})$ where the H_2 fraction is small (Savage et al. 1977). A regression fit to the data at $0.015 \leq E(\text{B-V}) \leq 0.07$ mag is $\log(y) = (0.100 \pm 0.016) + (0.960 \pm 0.011) \log(E(\text{B-V}))$ where $y = N(\text{H I})/5.8 \times 10^{21} \text{ cm}^{-2}$.

As shown at right there is a small non-zero y-intercept to a linear fit, $y = 0.00363 + 1.3581 E(\text{B-V})$ or $E(\text{B-V}) = -0.00267 + N(\text{H I})/7.87 \times 10^{21} \text{ cm}^{-2}$ which is very similar to an implicit result in Peek (2013), as noted here in Section 4.2.

A formal fit for the mean displacement between the regression lines and the canonical scaling is a factor 1.43, ie a mean slope $dN(\text{H I})/dE(\text{B-V}) = 8.3 \times 10^{21} \text{ cm}^{-2} E(\text{B-V})$. Note that the putative displacement cannot be discerned at $E(\text{B-V}) > 0.12$ mag, in part because the H_2 fraction is appreciable and partly because the optical depth at 21cm is not compensated in the attendant cooler gas.

As a check, Figure 2 shows that the reddening derived from the SFD98 datacubes is already larger than that of BH82, except over a narrow range at $0.06 < E(\text{B-V}) < 0.1$ mag. Recent suggestions for corrections to the SFD98 results (Schlafly et al. 2010; Schlafly & Finkbeiner 2011; Berry et al. 2012) imply an overall decrease of 10-15% in the SFD98 reddening that would somewhat ameliorate the differences between SFD98 and BH82 while increasing the value we derive for $N(\text{H I})/E(\text{B-V})$ by the same amount.

Given the behaviour in Figure 2 it is interesting to contemplate what Figure 1 would have looked like if had been constructed just before the appearance of SFD98. The reddenings of BH82 do not increase much beyond $E(\text{B-V}) = 0.2$ mag, so that the broad wing extending to high $E(\text{B-V})$ in Figure 1 would have been compressed and pushed back to the regression line. At small $E(\text{B-V})$ the reddening of BH82 declines much faster than that of SFD98, leading to high values of the gas/dust ratio as noted in Section 4.2.

Table 1 shows some summary properties for the data displayed in Figure 1. The southern sky consistently has 20-30% more gas at $|b| \geq 35^\circ$, a well-known aspect of galactic structure (Dickey & Lockman 1990). The $\text{H I}/E(\text{B-V})$ ratio is more consistent in the north but steadily increasing with $|b|$ in the south. Some part of that increase could be explained by colder gas and a stronger correction for saturation in the H I but it also appears that the extra gas in the south is not accompanied by a full complement of added reddening. In any case, Table 1 gives some idea of the expected variability in $N(\text{H})/E(\text{B-V})$ at/above 35° where the opacity correction is small; nearly none in the northern sky and 15-20

3.2. Smaller-scale results using GALFA HI

As a check on the wide-scale results from the LAB survey, we considered regions mapped at 4' resolution in the GALFA-HI survey of Peek et al. (2011). Shown in Figures 3 and 4 are results derived from two custom $5^\circ \times 5^\circ$ cubes delivered by the GALFA data server.

Figure 3 shows the $N(\text{H I}) - E(\text{B-V})$ comparison for a region at $b \approx -33^\circ$ that was specifically selected from a reddening map to avoid sightlines with $E(\text{B-V}) \gtrsim 0.1$. The formal value of the displacement of the data from the canonical scaling is a factor 1.53, slightly larger than in Figure 1.

Shown at left in Figure 4 are overlays of the reddening (in pseudo-color) and contours of the H I profile integral for a region specifically chosen to contain a wide range in reddening and portions of the high-latitude CO-emitting cloud MBM53 (Magnani et al. 1985). This part of the sky near the MBM53-55 complex harbors a relatively large H_2 -fraction even in regions where $E(\text{B-V}) \lesssim 0.1$ mag (Liszt & Pety 2012). Although the $E(\text{B-V})$ map and the contours of the H I profile integral correspond quite closely, the plot at right in Fig. 4 makes clear that the range of the H I column density is very much compressed compared to that of the reddening. The H I profiles are depressed by the presence of cold gas and a high molecular fraction at relatively small $E(\text{B-V})$ but $N(\text{H I})$ still lies well above the dashed line representing the canonical scaling between $N(\text{H})$ and $E(\text{B-V})$ at smaller values of $E(\text{B-V})$.

4. Discussion

4.1. Suggested corrections to SFD98

We noted in Section 3.1 and Figure 2 that the SFD98 results are generally larger than those of BH82. Schlafly & Finkbeiner (2011) and Schlafly et al. (2010) derived a 14% downward overall scaling of the SFD98 results and they and Berry et al. (2012) discuss corrections to the SFD98 reddening as well as a normalization difference between the north and south hemispheres of about 20%. Downward scaling of the SFD98 results would lessen some of the differences seen in Figure 2 while exacerbating the disparity in the $E(\text{B-V}) - N(\text{H I})$ comparison discussed here. Peek & Graves (2010) argued that the SFD98 reddening could be low by as much as 50% over limited portions of the sky where the dust temperature is low but generally confirmed the SFD98 values otherwise.

4.2. Prior uses of 21cm data

With respect to the radio data, the effect manifested in Figures 1, 3 and 4 is not subtle and it is perhaps surprising that it has not been previously called out. However, the effect can be found in the literature in various ways when it is sought; for instance Figure 4 of Abdo et al. (2010) where the SFD98 reddening is uniformly too small outside the molecular regions, compared to the canonically-scaled $N(\text{H I})$. This is as expected from the plot in Figure 1, showing the suppression of the H I profile integral for $E(\text{B-V}) > 0.1$ mag.

Peek (2013) related both $E(\text{B-V})$ and a scaled representation of the optically thin values of $N(\text{H I})$ to his galaxy-color-derived reddening measure over a wide region around the North Galactic Cap. The implied $E(\text{B-V})$ - $N(\text{H I})$ relationship from his equations 1 and 2 is $E(\text{B-V}) = -0.00243 + N(\text{H I})/7.64 \times 10^{21} \text{ cm}^{-2}$, very similar to the linear fit to the data shown in Figure 1, as noted in Section 3.1. At $E(\text{B-V}) = 0.06$ mag one has $N(\text{H I})/E(\text{B-V}) = 7.95 \times 10^{21} \text{ cm}^{-2}/\text{mag}$, tantamount to a 37% rescaling of the H I- $E(\text{B-V})$ ratio, compared to our fitted value of 43% using (lightly) optical-depth corrected $N(\text{H I})$ in Figure 1.

In the original discussion of Bohlin et al. (1978) it was noted that the slope of the $N(\text{H I})$ - $E(\text{B-V})$ relationship derived from contemporaneous 21cm H I measurements and galaxy counts was somewhat smaller, $dN(\text{H I})/dE(\text{B-V}) = 4.85 \times 10^{21} \text{ cm}^{-2} \text{ mag}^{-1}$ in Heiles (1976). This was consistent with the comparison between $E(\text{B-V})$ and $N(\text{H I})$ derived from the Ly- α line, see just below. However, although the slope was correctly quoted, the discussion of Bohlin et al. (1978) glosses over an important aspect of the regression fit derived by Heiles (1976), $E(\text{B-V}) = (-0.041 \pm 0.012) + N(\text{H I})/(4.85 \pm 0.36) \times 10^{21} \text{ cm}^{-2}$. Regardless of whether the negative intercept is physically-based, as Heiles (1976) suggested might be the case (ie, gas without dust), it reflects very large ratios $N(\text{H I})/E(\text{B-V})$ at low $E(\text{B-V})$, for instance $N(\text{H I})/E(\text{B-V}) = 8.2 \times 10^{21} \text{ cm}^{-2} \text{ mag}^{-1}$ at $E(\text{B-V}) = 0.06$ mag, quite in line with the present discussion.

4.3. $N(\text{H I})$ derived from Ly- α absorption

The $N(\text{H I})$ data of Bohlin et al. (1978) derived from Ly- α absorption are shown in Figure 5 and the behaviour is mostly opposite to that displayed in Figure 1 here. At lower $E(\text{B-V})$ the scatter is larger and the H I column densities are below $5.8 \times 10^{21} \text{ cm}^{-2} E(\text{B-V})$.

It was well understood that the sightlines selected for uv absorption measurements by *Copernicus* had low mean density and were biased toward lower H_2 -fractions (Bohlin et al. 1978). This in part explains the near coincidence of $N(\text{H I})$ and the canonical scaling of $E(\text{B-V})$ at $E(\text{B-V}) > 0.1$ mag in Figure 5, well beyond the point at which $E(\text{B-V})$ and $N(\text{H I})$ diverge in Figure 1. However, assuming a fixed gas/dust ratio, there would be no reason to correct the derived $N(\text{H I})/E(\text{B-V})$ for a

small H_2 fraction if both $N(H\ I)$ and $N(H_2)$ were accurately measured, no matter the sample biases.

The somewhat small values of $N(H\ I)/E(B-V)$ at $E(B-V) < 0.1$ mag in Figure 5 could be explained by adding a 15% contribution for hydrogen that is ionized along the sightlines to those early-type stars: Bohlin et al. (1978) quote $N(H\ I)/E(B-V) = 5 \times 10^{21} \text{ cm}^{-2} \text{ mag}^{-1}$. However, aligning the radio and uv results below $E(B-V) = 0.1$ mag in this same way would require a very large contribution from ionized gas, of order 60% of the observed $N(H\ I)$ derived from $Ly-\alpha$. Alternatively, the grains observed toward these stars may actually be different.

Diplas & Savage (1994) (see also Kim & Martin (1996)) used archival IUE spectra and expanded the sample of $N(H\ I)$ derived from $Ly-\alpha$ absorption by about a factor 5. They quote $N(H\ I)/E(B-V) = 4.93 \times 10^{21} \text{ cm}^{-2} \text{ mag}^{-1}$ at $E(B-V) > 0.1$ mag, just as in Bohlin et al. (1978). However, for $E(B-V) < 0.1$ mag their measurements give much higher $N(H\ I)/E(B-V)$, more in line with what we derive, and opposite to the data of Bohlin et al. (1978) shown here in Figure 5.

5. Summary and conclusions

We compared IR-derived measures of $E(B-V)$ and $N(H\ I)$ derived from wide-field $H\ I$ sky surveys at low ($36'$; Figure 1) and high ($4'$, Figures 3 and 4) spatial resolution in the 21 cm line and found a 40%-50% displacement between the resultant $N(H\ I)/E(B-V)$ ratio $\approx 8.3 \times 10^{21} \text{ cm}^{-2} \text{ mag}^{-1}$ and the usually-quoted scaling $N(H) = 5.8 \times 10^{21} \text{ cm}^{-2} E(B-V)$, at least at $E(B-V) \lesssim 0.1$ mag where the H_2 fraction is low and little saturation of the $H\ I$ profiles is evident. In any case, the commonly-cited systematic errors in deriving $N(H\ I)$ from the $H\ I$ profile, and the systematic deviations of $N(H)$ and $N(H\ I)$ to account for the contribution of ionized gas, would all increase the hydrogen column density and exaggerate the disparity between the two scaling relations.

Along the way we digressed to note that the IR dust emission-derived reddening is already larger than that derived from earlier all sky surveys of galaxy counts and that recent suggestions for recalibration of the reddening would lessen the disparity with earlier studies of galaxy counts but widen it with respect to our $H\ I$ measure. We showed that there have been intimations of a high 21 cm- $N(H\ I)/E(B-V)$ ratio for $E(B-V) < 0.1$ mag for some time but that a somewhat opposite effect was seen in $uv\ Ly-\alpha$ measurements of $N(H\ I)$ toward early-type stars.

There is no doubt that the gas column density and dust optical depth are well and, apparently, linearly correlated on large scales at $E(B-V) \lesssim 0.1$ mag, but the coefficient of proportionality seems to have been mis-estimated by a surprisingly large amount, for a surprisingly long while. If the FIR-derived $E(B-V)$ and 21 cm-derived $N(H\ I)$ have been measured correctly, they imply a 30% decrease in the accepted galactic $E(B-V)/N(H)$ ratio at $E(B-V) \lesssim 0.08$ mag where $N(H\ I) \approx N(H)$. Moreover, the obvious sources of possible error, opacity in the $H\ I$ and the unobserved contribution

of H II, both go in the direction of increasing the disparity. Conversely, if the stellar reddening and uv absorption measurements of H I and H₂ are also accurate, either a very large contribution from ionized gas was neglected toward the early-type stars or the dust optical depths per H-nucleus are larger than in the Galaxy at large.

In a subsequent paper we will discuss the physical reasons for the divergence between N(H I) and the linear E(B-V)-N(H I) scaling at E(B-V) < 0.1 mag. By considering the H I profiles and the established empirical relationship between E(B-V) and the integrated H I optical depth, it is straightforward to show that saturation of the 21cm line is much less important than the conversion of hydrogen atoms to H₂.

The National Radio Astronomy Observatory is operated by Associated Universities, Inc. under a contract with the National Science Foundation. The author was partially funded by the grant ANR-09-BLAN-0231-01 from the French *Agence Nationale de la Recherche* as part of the SCHISM project (<http://schism.ens.fr/>). The author acknowledges the hospitality of Newrest at the ALMA OSF facility at 2800m in the Atacama and the hospitality of the Hotel Director in Santiago during the writing of this manuscript. I thank Bruce Draine for words of encouragement and I thank the referee, Josh Peek, for his helpful remarks.

This publication utilized Galactic ALFA HI (GALFA HI) survey data obtained with the Arecibo L-band Feed Array (ALFA) on the Arecibo 305m telescope. The GALFA HI surveys are funded by the NSF through grants to Columbia University, the University of Wisconsin, and the University of California.

REFERENCES

- Abdo, A. A., Ackermann, M., Ajello, M., Baldini, L., Ballet, J., Barbiellini, G., Bastieri, D., Baughman, B. M., Bechtol, K., Bellazzini, R., Berenji, B., Bloom, E. D., Bonamente, E., Borgland, A. W., Bregeon, J., Brez, A., Brigida, M., Bruel, P., Burnett, T. H., Buson, S., Caliandro, G. A., Cameron, R. A., Caraveo, P. A., Casandjian, J. M., Cecchi, C., Celik, Ö., Chekhtman, A., Cheung, C. C., Chiang, J., Ciprini, S., Claus, R., Cohen-Tanugi, J., Cominsky, L. R., Conrad, J., Dermer, C. D., de Palma, F., Digel, S. W., Silva, E. d. C. e., Drell, P. S., Dubois, R., Dumora, D., Farnier, C., Favuzzi, C., Fegan, S. J., Focke, W. B., Fortin, P., Frailis, M., Fukazawa, Y., Funk, S., Fusco, P., Gargano, F., Gehrels, N., Germani, S., Giavitto, G., Giebels, B., Giglietto, N., Giordano, F., Glanzman, T., Godfrey, G., Grenier, I. A., Grondin, M.-H., Grove, J. E., Guillemot, L., Guiriec, S., Harding, A. K., Hayashida, M., Horan, D., Hughes, R. E., Jackson, M. S., Jóhannesson, G., Johnson, A. S., Johnson, W. N., Kamae, T., Katagiri, H., Kataoka, J., Kawai, N., Kerr, M., Knödlseder, J.,

- Kuss, M., Lande, J., Latronico, L., Lemoine-Goumard, M., Longo, F., Loparco, F., Lott, B., Lovellette, M. N., Lubrano, P., Makeev, A., Mazziotta, M. N., McEnery, J. E., Meurer, C., Michelson, P. F., Mitthumsiri, W., Mizuno, T., Monte, C., Monzani, M. E., Morselli, A., Moskalenko, I. V., Murgia, S., Nolan, P. L., Norris, J. P., Nuss, E., Ohsugi, T., Okumura, A., Omodei, N., Orlando, E., Ormes, J. F., Paneque, D., Pelassa, V., Pepe, M., Pesce-Rollins, M., Piron, F., Porter, T. A., Rainò, S., Rando, R., Razzano, M., Reimer, A., Reimer, O., Reposeur, T., Rodriguez, A. Y., Ryde, F., Sadrozinski, H. F.-W., Sanchez, D., Sander, A., Saz Parkinson, P. M., Sgrò, C., Siskind, E. J., Smith, P. D., Spandre, G., Spinelli, P., Starck, J.-L., Strickman, M. S., Strong, A. W., Suson, D. J., Takahashi, H., Tanaka, T., Thayer, J. B., Thayer, J. G., Thompson, D. J., Tibaldo, L., Torres, D. F., Tosti, G., Tramacere, A., Uchiyama, Y., Usher, T. L., Vasileiou, V., Vilchez, N., Vitale, V., Waite, A. P., Wang, P., Winer, B. L., Wood, K. S., Ylinen, T., Ziegler, M., & Fermi/LAT Collaboration. 2010, *ApJ*, 710, 133
- Berry, M., Ivezić, Ž., Sesar, B., Jurić, M., Schlafly, E. F., Bellovary, J., Finkbeiner, D., Vrbanec, D., Beers, T. C., Brooks, K. J., Schneider, D. P., Gibson, R. R., Kimball, A., Jones, L., Yoachim, P., Krughoff, S., Connolly, A. J., Loebman, S., Bond, N. A., Schlegel, D., Dalcanton, J., Yanny, B., Majewski, S. R., Knapp, G. R., Gunn, J. E., Allyn Smith, J., Fukugita, M., Kent, S., Barentine, J., Krzesinski, J., & Long, D. 2012, *ApJ*, 757, 166
- Bohlin, R. C., Savage, B. D., & Drake, J. F. 1978, *ApJ*, 224, 132
- Burstein, D. & Heiles, C. 1982, *Astron. J.*, 87, 1165
- Dame, T. M., Hartmann, D., & Thaddeus, P. 2001, *ApJ*, 547, 792
- Dickey, J. M. & Lockman, F. J. 1990, *Ann. Rev. Astr. Ap.*, 28, 215
- Diplas, A. & Savage, B. D. 1994, *ApJ*, 427, 274
- Heiles, C. 1976, *ApJ*, 204, 379
- Heiles, C. & Troland, T. H. 2003, *ApJ*, 586, 1067
- Kalberla, P. M. W., Burton, W. B., Hartmann, D., Arnal, E. M., Bajaja, E., Morras, R., & Pöppel, W. G. L. 2005, *A&A*, 440, 775
- Kim, S.-H. & Martin, P. G. 1996, *ApJ*, 462, 296
- Liszt, H. & Lucas, R. 2002, *A&A*, 391, 693
- Liszt, H. S. & Pety, J. 2012, *A&A*, 541, A58

- Liszt, H. S., Pety, J., & Lucas, R. 2010, *A&A*, 518, A45
- Magnani, L., Blitz, L., & Mundy, L. 1985, *ApJ*, 295, 402
- Peek, J. E. G. 2013, *ApJ*, 766, L6
- Peek, J. E. G. & Graves, G. J. 2010, *ApJ*, 719, 415
- Peek, J. E. G., Heiles, C., Douglas, K. A., Lee, M.-Y., Grcevich, J., Stanimirović, S., Putman, M. E., Korpela, E. J., Gibson, S. J., Begum, A., Saul, D., Robishaw, T., & Krčo, M. 2011, *Astrophys. J., Suppl. Ser.*, 194, 20
- Planck Collaboration, Ade, P. A. R., Aghanim, N., Arnaud, M., Ashdown, M., Aumont, J., Baccigalupi, C., Balbi, A., Banday, A. J., Barreiro, R. B., & et al. 2011, *A&A*, 536, A19
- Savage, B. D., Drake, J. F., Budich, W., & Bohlin, R. C. 1977, *ApJ*, 216, 291
- Schlafly, E. F. & Finkbeiner, D. P. 2011, *ApJ*, 737, 103
- Schlafly, E. F., Finkbeiner, D. P., Schlegel, D. J., Jurić, M., Ivezić, Ž., Gibson, R. R., Knapp, G. R., & Weaver, B. A. 2010, *ApJ*, 725, 1175
- Schlegel, D. J., Finkbeiner, D. P., & Davis, M. 1998, *ApJ*, 500, 525
- Spitzer, L. 1968, *Diffuse matter in space* (New York: Interscience Publication, 1968)

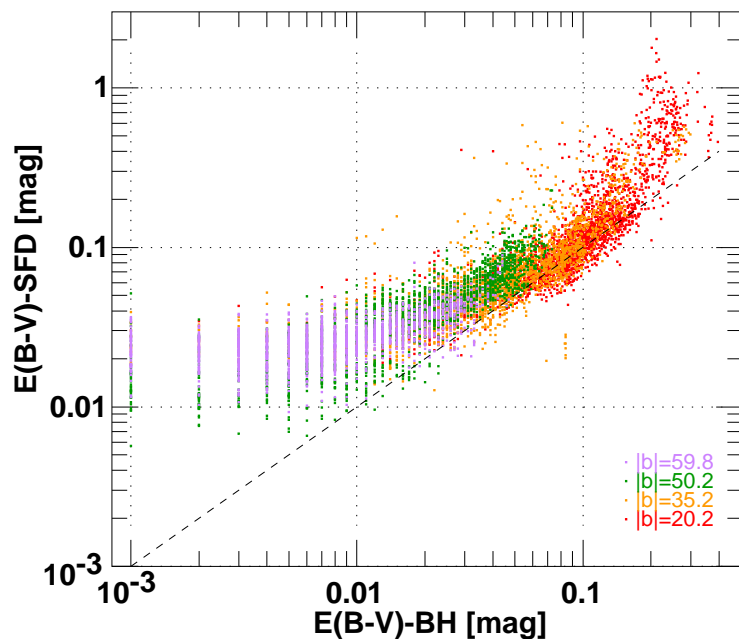


Fig. 2.— Reddening $E(B-V)$ derived from the datasets of SFD98 and BH82 along tracks that most closely approximate those used to create Figure 1. The reddening was sampled at all 1200 longitude grid-points of the BH82 dataset at positive and negative values of the latitudes indicated.

Table 1: Mean quantities for the data displayed in Figure 1

b	$\langle \int T_B dv \rangle$ K-km s $^{-1}$	$\langle E(B-V) \rangle$ mag	$\langle \int T_B dv \rangle / \langle E(B-V) \rangle^a$ cm $^{-2}$ mag $^{-1}$
-60°	124	0.0238	9.92×10^{21}
60°	102	0.0234	8.13×10^{21}
-50°	178	0.0431	8.61×10^{21}
50°	136	0.0318	8.31×10^{21}
-35°	312	0.0951	7.36×10^{21}
35°	252	0.0633	8.07×10^{21}
-20°	439	0.1821	6.55×10^{21}
20°	412	0.1569	7.14×10^{21}

^a rescaled by 1.823×10^{18} cm $^{-2}$ to give optically thin N(H I)

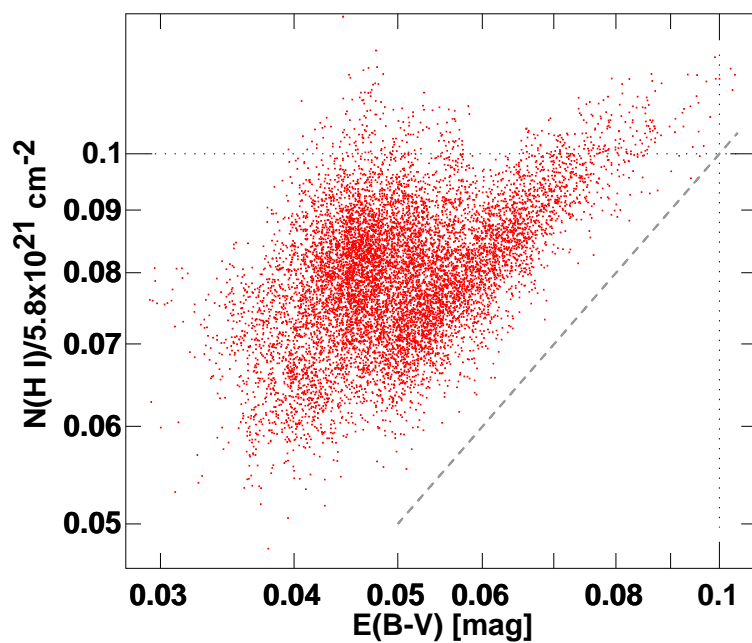


Fig. 3.— Reddening from SFD98 and $N(\text{H I})$ from the GALFA survey at $4'$ resolution corrected for a spin temperature of 145 K, in a 5° field centered at $\text{RA}(\text{J2000}) = 18\text{h}30\text{m}$, $\text{Dec}(\text{J2000}) = 22^\circ30'$ ($l = 82.099^\circ$, $b = -32.931^\circ$) chosen to avoid sightlines at $E(\text{B-V}) > 0.1$ mag. The dashed line is the canonical scaling $N(\text{H I}) = 5.8 \times 10^{21} \text{ cm}^{-2} E(\text{B-V})$, as in Figure 1.

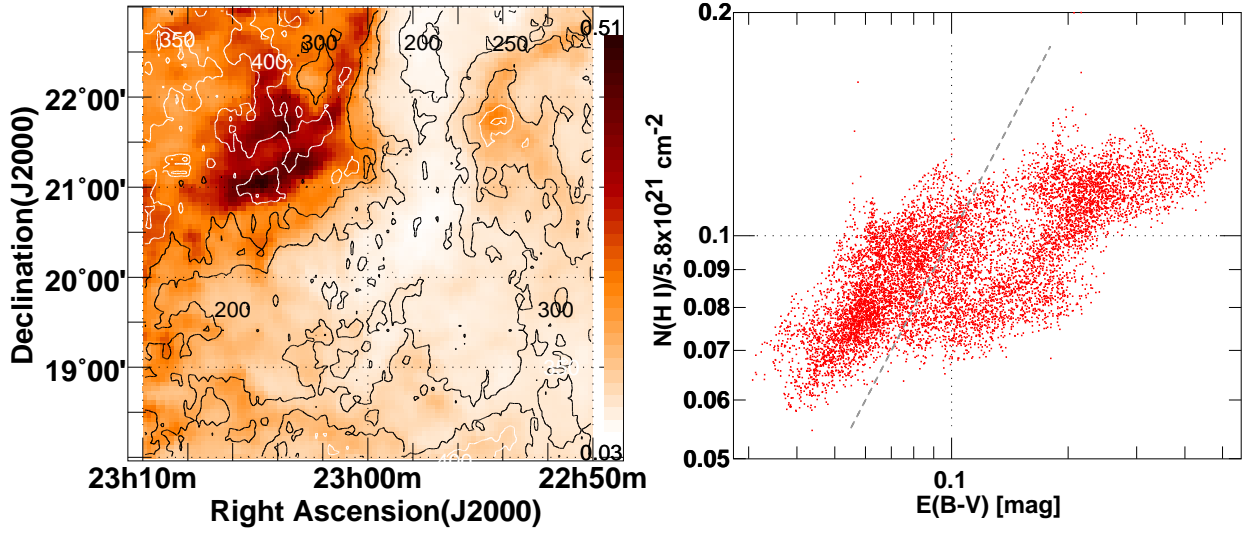


Fig. 4.— Reddening and H I in a 5° field centered at RA(J2000) = 23h, Dec(J2000) = $20^\circ 30'$, near the high-latitude molecular cloud MBM53. Left: Pseudo-color map of reddening $E(B-V)$ ($0.03 < E(B-V) < 0.51$ mag) with overlaid contours of the H I profile integral (units of K-km s^{-1}) using $4'$ -resolution HI data from the GALFA survey. Right: plot of $N(\text{H I})$ corrected for optical depth using a spin temperature of 145 K vs. reddening. The dashed line is the canonical scaling $N(\text{H I}) = 5.8 \times 10^{21} \text{ cm}^{-2} E(B-V)$, as in Figure 1.

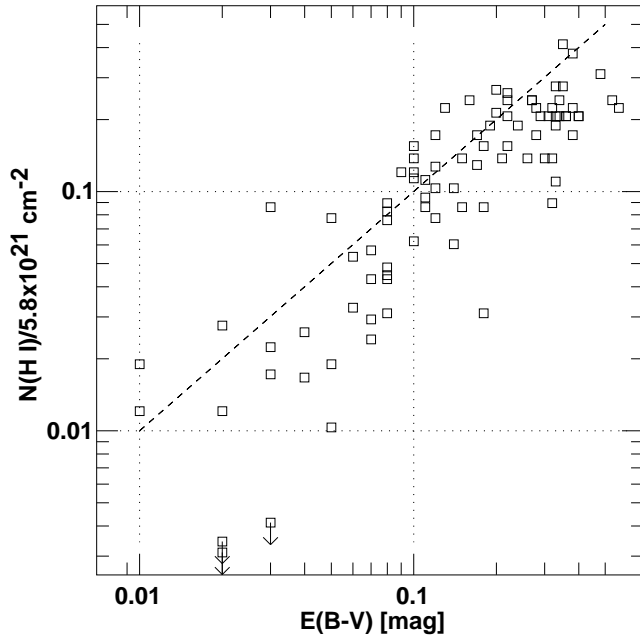


Fig. 5.— Stellar reddening and $N(\text{H I})$ derived from $\text{Ly-}\alpha$ measurements by Bohlin et al. (1978).